Optimization of anti-reflective coatings for lithography applications

J. Bauer, O. Fursenko, S. Virko*, B. Kuck, Th. Grabolla, V. Melnik, W. Mehr

IHP, Im Technologiepark 25, 15236 Frankfurt (Oder), Germany
bauer@ihp-microelectronics.com
*Institute of Semiconductor Physics (ISP) of Nat. Acad. Sci. of Ukraine,
41, Pr. Nauky, Kyiv, 03028, Ukraine

Abstract

We present a new multilayer anti-reflective coating (ARC) optimization method. We have developed a software which allows the optimization of ARC consisting of up to 20 layers on any substrate with incident light integration over the aperture of lithography objectives and diffraction effects. The optimization includes not only the determination of optimal layer parameters (i.e. optical constants n and k, and thickness d) for minimized back-to-resist reflection (R_{12}) of exposing light but also the determination of appropriate intervals of parameters corresponding to values smaller then desired values of R_{12}. By this way the calculation of the process window of technological parameters is essentially improved. The optimization procedure delivers the process parameter for the deposition process determining the characteristics for the ARC layer, namely flow ratio of the source gases, for different ARC layers using optical constants obtained by spectroscopic ellipsometry and reflection spectroscopy.

Based on these results the optical constants, thickness and corresponding compositions of low pressure (LP) chemical vapor deposition (CVD) silicon-rich nitride (SiN_x), plasma-enhanced (PE) CVD silicon-rich nitride (SiN_x), and silicon-rich oxynitride (SiN_xO_y) were obtained. The optimized films fulfill the anti-reflective requirements for ArF (λ=193 nm), KrF (λ=248 nm) laser and i-line (λ=365 nm) lithography. X-ray photoelectron spectroscopy was applied for determination of the film composition. As an example, results of single layer ARC optimization for gate film stack and multi layer ARC optimizations for emitter window and metallization film stack are presented.

1. Introduction

The well-known thin-film interference effect in photoresist is caused by reflection from the substrate which is determined by the optical constants of the photoresist materials and substrates [1]. The interference effect leads to a variation of absorbed energy in the resist, which results in a strong fluctuation of line width. In order to prevent this line width fluctuations, the reflectivity in to the resist should be minimized by using high-performance anti-reflective coatings (ARC), which can be easily matched to the actual device process [2-4].

Silicon oxynitride (SiO_yN_x) [5]-[11] and silicon-rich nitride (SiN_x) [11] are very useful ARC materials, whose n and k values lie between the refractive indices of Si, SiO_2 and Si_3N_4 and are tunable by changing the composition (x, y).

For these materials we had optimized the antireflective multilayer systems for high-resolution lithography with high numerical aperture of the lithography lens (NA), high illumination aperture (NA_{ill}), under consideration of the diffraction effect.

2. ARC materials (SiN_x and SiN_xO_y) characterization

PECVD SiN_x and SiN_xO_y layers were deposited using a parallel-plate system CENTURA (Applied Materials Inc.) at 400°C with different SiH_4/N_2O and SiH_4/NH_3 gas flow ratios (GFR). The LPCVD SiN_x layers were deposited in a standard vertical batch system A400

(ASM Inc.) at ≥ 700°C with variable SiH_2Cl_2/NH_3 GFR. The films were deposited on *p*-type Si (100) wafers.

X-ray photoelectron spectroscopy (XPS) measurements performed by PHI 5600 tool were applied for composition characterization. Spectroscopic ellipsometry (SE) and reflection spectrometry were used for the determination of optical constants *n* and *k*. These measurements were done using automated spectroscopic ellipsometer UV1280 (KLA-TENCOR) in the wavelength range of 240-800 nm and OPTIPROBE (Therma-Wave Ltd.) in the wavelength range from 190-800 nm. For determination of the ARC dispersion models the thicknesses were additionally verified by X-ray reflection analysis.

Figure 1 shows the refractive indices *n*, *k* vs. GFR for LPCVD SiN_x (a), PECVD SiN_x (b) and PECVD SiO_xN_y. Evaluating the data presented in Fig. 1 for constant wavelength (193, 248 and 365 nm) analogous Fig. 6 the following results has been obtained. The refractive indices are strongly affected by the mole ratio in the source gas. For all materials we found that increasing of the silicon components (SiH_4 or SiH_2Cl_2) in the GFR the red shift of absorption edge is observed. At the wavelengths of 193 nm and 248 nm the real part *n* first increases with increasing silicon portion. For higher silicon portions *n* decreases because the relatively small refractive index of Si becomes more and more dominating.

Fig. 2 presents the composition obtained by XPS as function of the GFR . With increasing of SiH_4 or SiH_2Cl_2 component the content of the silicon increases. SiN_xO_y films show an increasing silicon content accompanied by decreasing oxygen and relatively constant nitrogen content with increasing SiH_4 (Fig. 2).

This is in correlation to the optical properties (Fig. 1). The optical data indicate a material with decreasing optical gap which is caused by the increased Si content [12], [13]. The result can be explained taking into consideration more Si-Si bonds and by this, diminishing structural disorder [12], [14], and a lower number of Si-O-Si bonds [11].

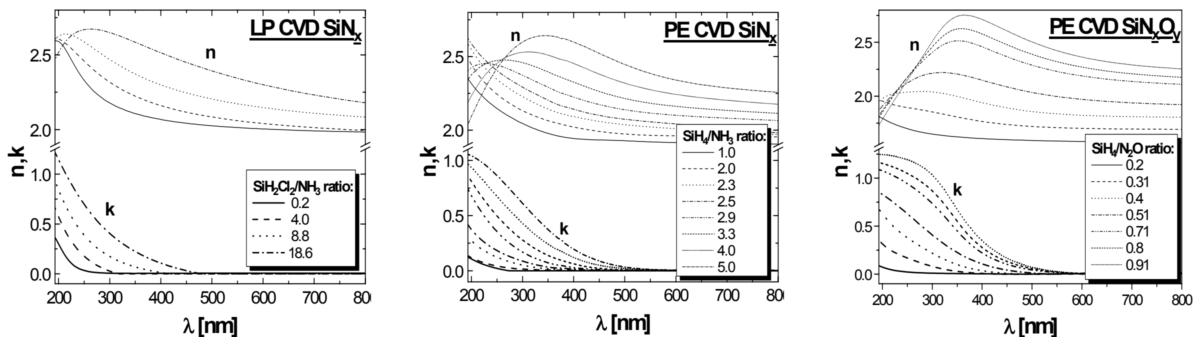

Fig. 1. Optical parameters (*n* and *k*) vs. wavelength (λ) for SiN_x-based ARC materials

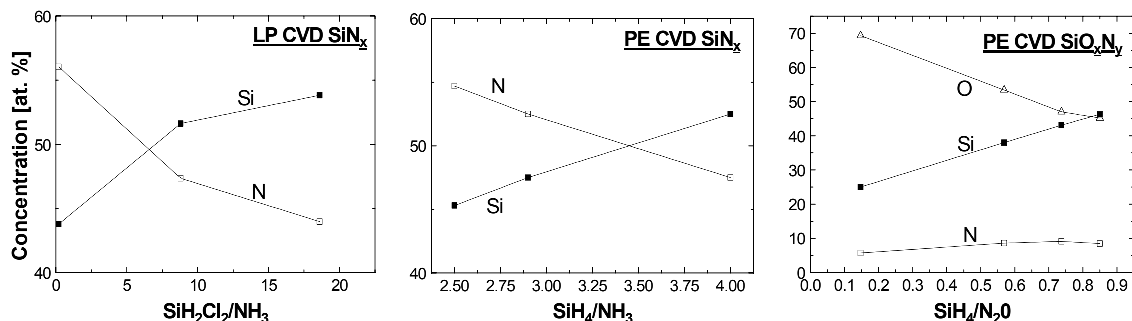

Fig. 2. The atomic concentrations of Si, N and O measured by XPS vs. gas flow ratios for SiN_x-based ARC materials

3. ARC Optimization Method

The software has been developed to calculate the reflectance of the resist surface (R_{01}) and the reflection from the interface resist/substrate (R_{12}) by using the matrix method based on the **Maxwell**'s equations [15, 16].
Assuming that the angle of incidence $\alpha+\alpha'$ caused by the optical system and the object diffraction is determined by the field in the pupil (Fig.3), it can be shown that the electric field weighted reflection is given by equation:

$$R_{i\,s,p} = \int_{Source}\int_{Pupil} |F\{U_{s,p}(x)\}|^2\ I_{s,p}(\alpha)\ R'_{i\,s,p}(\alpha'+\alpha)\ d\alpha' d\alpha \Big/ \int_{Source}\int_{Pupil} |F\{U_{s,p}(x)\}|^2\ I_{s,p}(\alpha)\ d\alpha' d\alpha, \quad (1)$$

where $R'_{i\,s,p}(\alpha'+\alpha) = |r'_{is,p}|^2$.

The imaging process of the object field in the pupil can be described as Fourier transforms $F\{U_{s,p}(\boldsymbol{x})\}$, according to **Hopkins**'s image model [17]. This process is illustrated by Fig. 3. If the diffraction is low (such as single line) or the coherence parameter $\sigma \approx 1$ ($\sigma = NA_{ill} / NA = \rho_{ill}/\rho_{pup}$, NA: lens aperture, NA_{ill}: illumination aperture) we can neglect the diffraction:

$$R_{i\,s,p} = \int_{Source} I_{s,p}(\alpha)\ R'_{i\,s,p}(\alpha) d\alpha \Big/ \int_{Source} I_{s,p}(\alpha) d\alpha \quad (2)$$

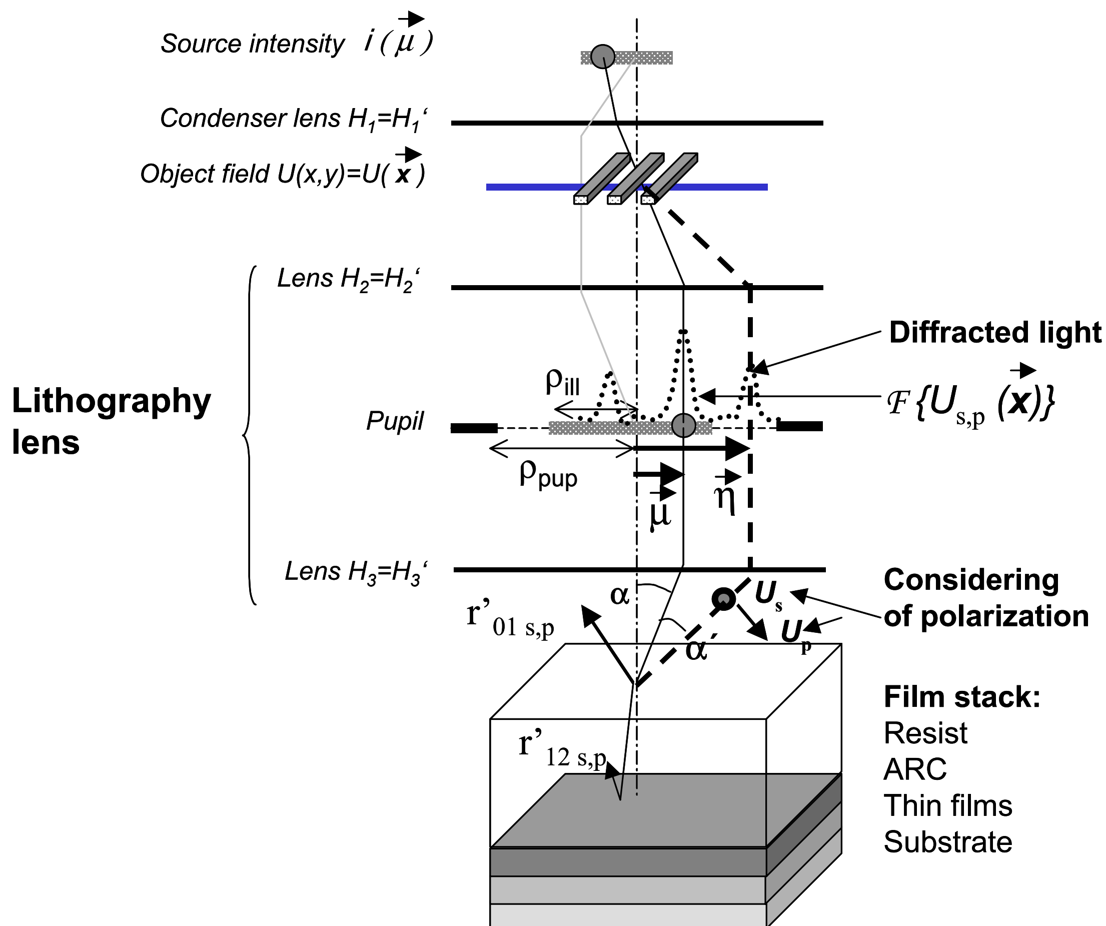

Fig. 3. Illustration of the optical system considering angle of incidence, polarization and diffraction.

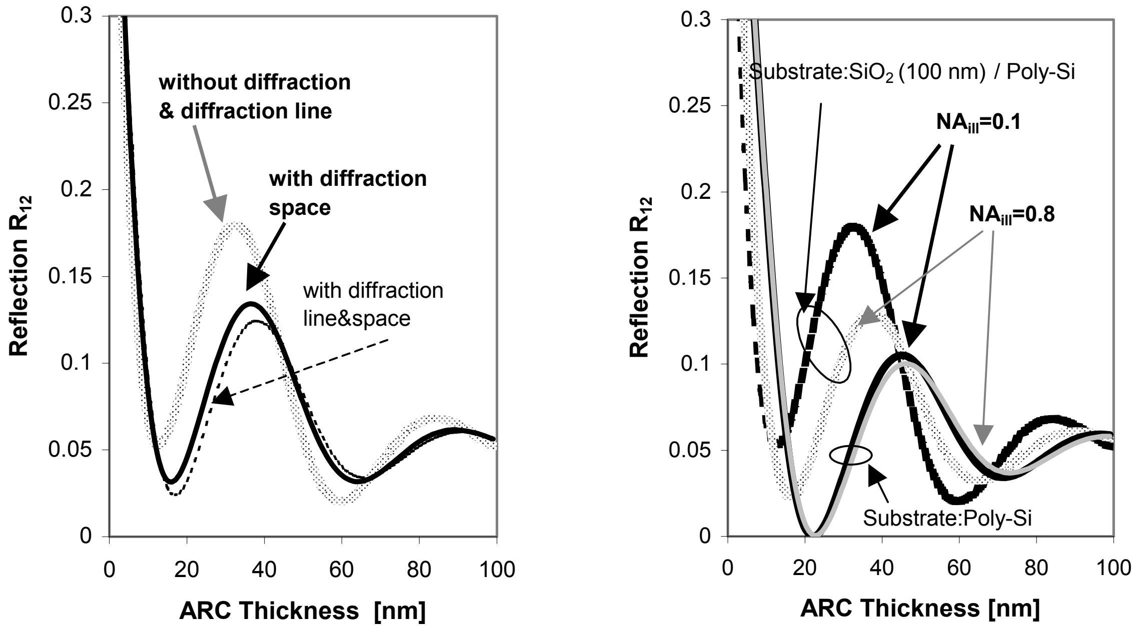

a) b)

Fig. 4. Interface resist/substrate reflection (R_{12}) vs. ARC (n=2.45, k=0.68) thickness at λ=248.4 nm (Resist UV210: n=1.757, k=0.0095):
a) R_{12} obtained by Eq. (1) without and with consideration of 0.18µm line and spaces diffraction (NA=0.9, NA_{ill}=0.1, substrate: SiO_2 (100 nm) /Poly-Si);
b) R_{12} obtained by Eq. (2) (NA=0.9, NA_{ill}=0.1 and 0.8, substrates: SiO_2 (100 nm) / Poly-Si and Poly-Si).

Fig. 4 shows some important results of R_{12} vs. ARC thickness simulations. When using SiO_2 below the ARC the reflection minimum is clearly shifted. Variation of diffraction by using different mask structures does influence the minimum position, too (Fig. 4a). Also NA_{ill} affects the minimum position, whereas no markedly effect is observed for oxide-free layer stack (Fig. 4b). Generally, diffraction and NA_{ill} have to be considered for relatively thick interference capable layers such as ARC, SiO_2 and/or Si_3N_4 films.
The software allows the optimization of ARC consisting of up to 20 layers on any substrate. The optimization includes not only the determination of optimal layer parameters (i.e. optical constants n and k, and thickness d) for minimized back-to-resist reflection (R_{12}) of exposing light but also the determination of appropriate intervals of parameters corresponding to values smaller then desired values of R_{12}. By this way the calculation of the process window of technological parameters is essentially improved. The optimization procedure delivers the process parameter for the deposition process determining the characteristics for the ARC layer, namely flow ratio of the source gases, for different ARC layers based on measurements of optical constants.

4. Results

4.1. Gate Stack ARC optimization for KrF lithography (λ=248.4 nm)

Fig.6 shows the measured k as function of n for KrF light exposure for different ARC materials (LPCVD SiN_x, PECVD SiN_x and PECVD SiN_xO_y) which were prepared by varying the GFR during deposition. The simulated curves of optical constants are also shown in this figure for the 1st and 2nd interference order minimum (as example, see Fig.7) with intervals of tolerance corresponding the R_{12}<1% for the gate stack (Fig.5).

The crossing points of simulated 1st and 2nd order reflection interference minimum with the measured *k(n)* curves are the optimal optical solutions. The first order optimum of optical parameters for ARC layers are marked (**x**) in Fig.6 and presented in Table 1. For example, for PECVD SiN_x we estimated a process window for R_{12}<1%: 2.45<n_{ARC}<2.48, 0.52<k_{ARC}<0.88, 3.3<*GFR*<5, 20nm<d_{ARC}<26nm.

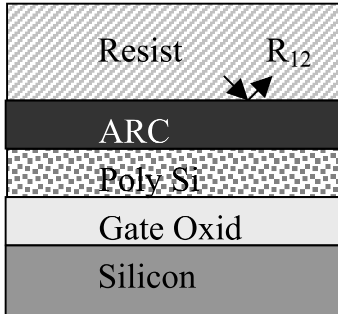

Fig. 5. Schematic cross section of the gate stack.

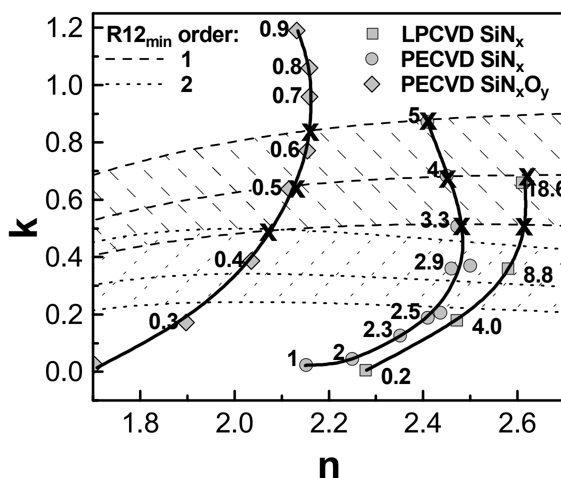

Fig. 6. Measured *k* values as function of *n* for different ARC materials obtained at different *GFR*, and simulated *k*(*n*) for 1st-2nd interference order of R_{12min} with intervals of tolerance R_{12}<1% for gate stack. (*NA*=0.82, σ=0.85 λ=248.4nm).

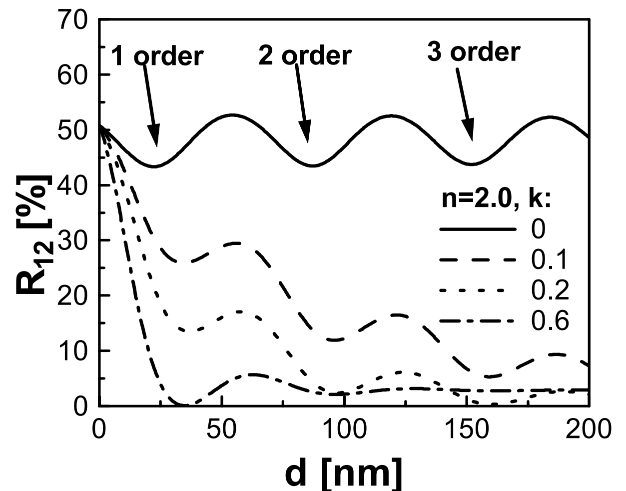

Fig. 7. R_{12} vs. *d*(ARC) at λ=248.4 nm for gate stack. Resist UV210: *n*=1.757, *k*=0.0095

Table 1: Optimization results for different ARC films on gate film stack for 248.4nm lithography (*NA*=0.82, σ=0.85).

ARC layer	*n*(ARC)	*k*(ARC)	*d*(ARC) nm	*Si* %	*O* %	*N* %	gas flow ratio
ARC optimum	*2.31*	*0.67*	*25.4*	-	-	-	-
LPCVD SiN_x	2.6	0.68	20	54	-	44	SiH_2Cl_2/NH_3 = 18.6
PECVD SiN_xO_y	2.12	0.647	30	34	52	16	SiH_4/N_2O = 0.5
PECVD SiN_x	2.45	0.68	23	52.5	-	47.5	SiH_4/NH_3 = 4

4.2. Gate stack ARC optimization for ArF lithography (λ=193 nm)

Fig. 8 shows optimal optical constants of PECVD SiN_xO_y layers (n=1.94, k=0.68, d=23nm) for ArF light exposure and the 1st order solutions for conventional optics for minimum back reflection in the resist R_{12min} for gate stack (Fig. 5). The influence of the immersion for conventional illumination (optimal optical constants of PECVD SiN_xO_y layers: n=1.96, k=0.63, d=25nm) and annual illumination (NA_{ill}=2/3annular, optimal optical constants of PECVD SiN_xO_y layers: n=1.96, k=0.59, d=26nm) are demonstrated too.

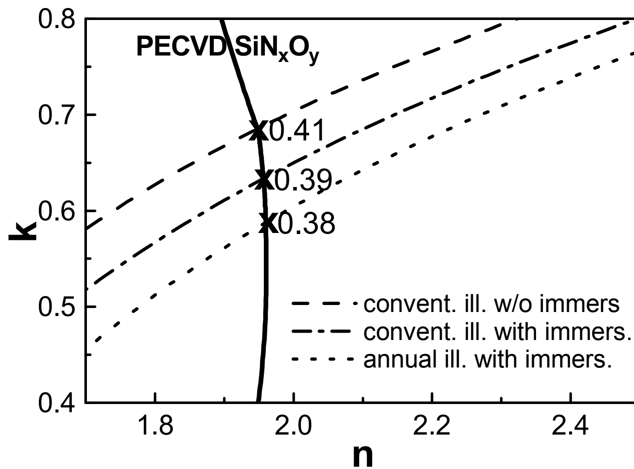

Fig. 8. Measured k vs. n at wavelength 193 nm for PECVD SiN_xO_y deposited at different GFR, and simulated $k(n)$ for 1st interference order of R_{12min} for gate stack (Resist/ARC/poly-Si).
Resist: n=1.7, k=0.01 (λ=193nm, NA=0.9 and NA=1.3(immersion), σ=0.85)

4.3. Multilayer ARC optimization for metallization stack for KrF lithography

Figure 10 and Table 2 show the 1st order R_{12} reflection minimum of metallization film stack (Fig. 9) with different ARC materials for KrF light exposure as an example of 3 layers optimization. The Ti and TiN thicknesses and the ARC layer parameters were optimized. The solution for theoretical ARC optimum is presented too.

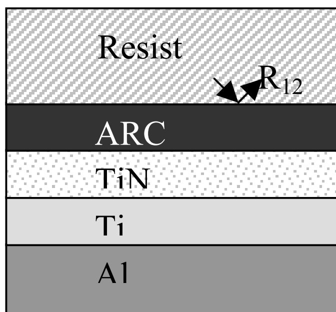

Fig. 9. Schematic cross section of the metallization stack.

Table 2: Optimization results for different ARC films on metallization film stack.

ARC layer	n(ARC)	k(ARC)	d(ARC) nm	d(TiN) nm	d(Ti) nm	gas flow ratio
ARC optimum	*2.22*	*0.31*	*22.0*	*15.5*	*21.5*	-
PECVD SiN_xO_y	2.02	0.35	29.5	14.5	20	SiH_4/N_2O = 0.39
PECVD SiN_x	2.44	0.24	17	16.5	21	SiH_4/NH_3 = 2.7

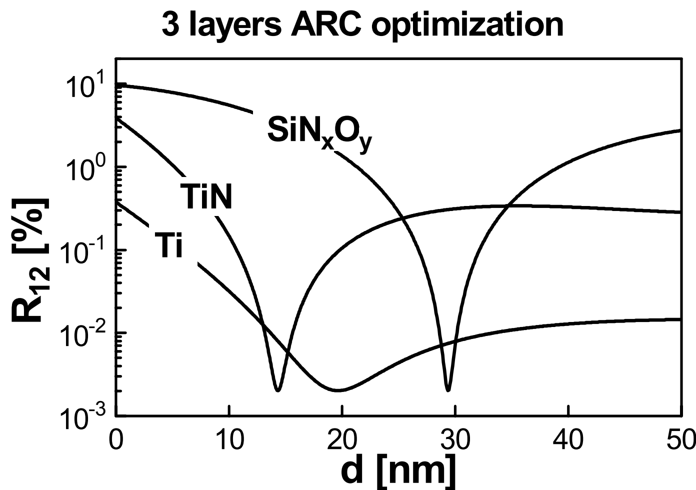

Fig. 10. R_{12} vs. thickness d for 3 layer metallization stack (resist UV210 / SiN_xO_y / TiN / Ti / Al) optimization.
(NA=0.82, σ=0.85, λ=248.4nm).

4.4. Multilayer ARC optimization for emitter window for KrF lithography

For IHP SiGe:C BiCMOS technology we optimize two layers (ARC and SiO_2) for emitter window patterning. The film stack is shown in Fig. 11.
The reflection is influenced by two interference capable layers shown in Fig. 12. The ARC effect is clearly visible for PECVD SiN_x (GFR=4) containing layer stack in contrast to the stack containing stoichiometric Si_3N_4 without antireflective behavior. The thickness optimization and the process window results are illustrated by contour maps, shown in Fig 13. The process window for the thickness is reduced for lower allowed back reflection.

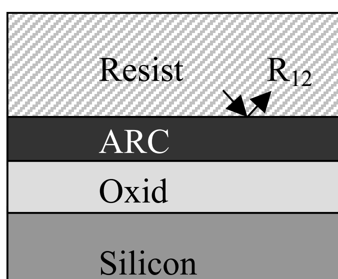

Fig. 11. Schematic cross section of Emitter window stack

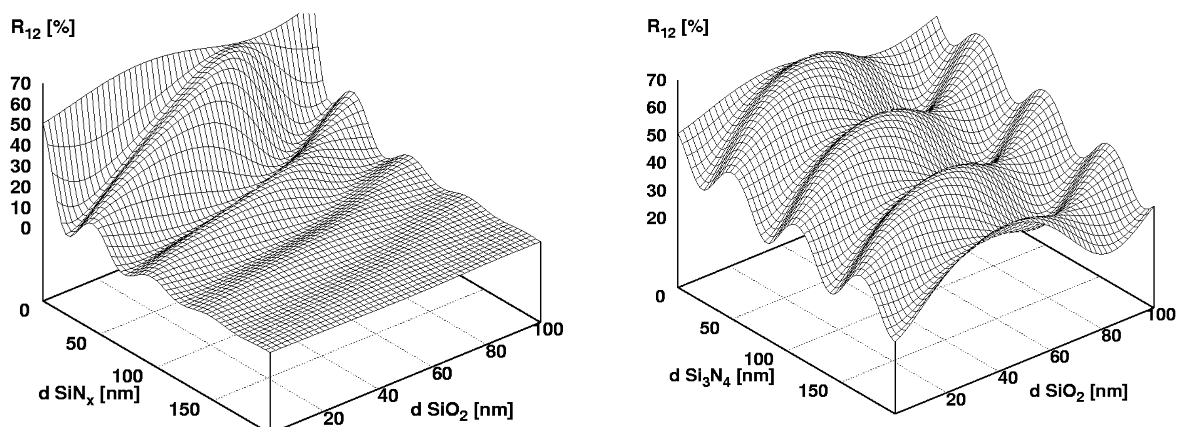

Fig. 12. Substrate reflectivity R_{12} vs. the SiO_2 and SiN_x thickness (a) and stoichiometric Si_3N_4 thickness (non ARC effect) (b)

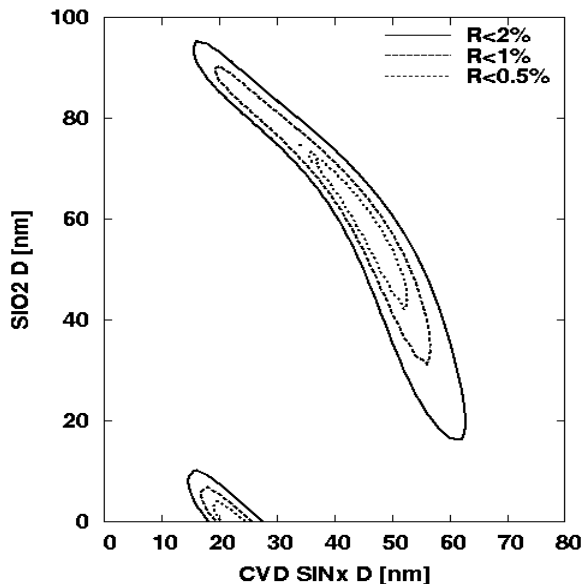

Fig. 13. Reflectivity contour map of PECVD SiN_x at *GFR*=4 for R_{12}≤0.5%, 1% and 2% as typical value for an excellent ARC.
Optical system: *NA*=0.82, σ=0.85, λ=248.4nm

5. Summary

We have developed an optimization method for a high performance ARC, which considers the optical system of lithography inclusive the diffraction effect. Our developed software allows to optimize a multi-layer ARC film stack and to calculate the process window of technological parameters for defined back-to-resist reflection.
As an application we showed single film ARC optimization for the gate stack for the KrF and ArF excimer lithography and multi-layer optimization for emitter window and metallization stacks. Our optimizer is well suited for designing multi-component ARC layers.

References

[1] T.A. Brunner, "Optimization of optical properties of resist process", SPIE, Vol. 1466 Advances in Resist technology and processing VIII, (1991) pp. 297–308.

[2] T. Ogawa, M. Kimura, Y. Tomo, and T. Tsumori, "Novel ARC Optimization Methodology for KrF Excimer Laser Lithography at Low K1 Factor", SPIE, 1674 Optical/Laser Microlithography V (1992) 362–375.

[3] Chr. Bencher, Chr. Nagai, B. Roman, S. Lian, and T. Vuong, " Dielectric antireflective coatings for DUV lithography, Solid state Technology, March 1997, 109–114.

[4] J. Bauer, G. Drescher, U. Jagdhold, U. Haak, Th. Skaluoud, " ARC technology to minimize CD-Variation during Emitter structuring-Experiment and Simulation", SPIE, Optical Microlithography XII, 3679 (1999) 106–116.

[5] T. Ogawa, A. Sekiguchi, N. Yoshizawa, "Advantages of a SiO_xN_y:H Anti-Reflective Layer for ArF Eximer Laser Lithography", Jpn. J. Appl. Phys., 35 (1996) 6360–6365.

[6] T. Ogawa, H. Nakano, T. Gocho, T. Tsumori, "SiO_xN_y:H, high performance anti-reflective layer for the current and future optical lithography", SPIE, 2197 Optical/Laser Microlithography VII (1994) 722–732.

[7] G. Chao, P.-Y. Lu, A. Ku, E. Mao, S. Chang, and R. Tang, "Improvement of using Dielectric Anti-Reflective coating (D-ARC) on Photo CD Control for ULSI Application", February 8-9, 1999 DUMIC Conference, 1999 IMIC-444D/99/0119.

[8] A. Kant, J.Yota, G. Talor, “Advatage Inorganic Anti-Reflective Coating PECVD SiO_xN_y for Sub-0.25µm Gate Lithography and Etch Processes”, February 8-9, 1999 DUMIC Conference, 1999 IMIC-444D/99/0127.

[9] J. Flicstein, J. Mba, B. Lescaut, Y.Vitel, P. Ossart, C. Licoppe, “SiNO large area deposition with a deep-UV flash argon/krypton lamp array”, Applied Surface Science, 106 (1996) 44–50.

[10] W.W. Lee, Q. He, A. Chatterjee, G. Xing, K. Brennan, A. Singh, E. Zielinski, M. Hanratty, S. Fang, D. Rogers, G. Dixit, D. Carter, J.D. Luttmer, B. Havemann, and R.A. Chapmann, “ARC for sub-0.18µm logic and gigabit DRAM. Frontend and backend processes”, IEEE, 1998, 86–87.

[11] M. Modreanu, N. Tomozeiu, P. Cosmin, M. Gartner, ”Physical-optical Properties of LPCVD Amorphous Silicon Rich-Nitride and Oxinidride”, IEEE, 1998, 201–204.

[12] M.I. Alayo, I. Pereyra, W.L. Scopel, M.C.A. Fantini, “On the Nitrogen and Oxygen Incorporation in Plasma-Enhanced chemical Vapor Deposition (PECVD) SiO_xN_y films”, Thin Solid Films 402 (2002) 154–161.

[13] C. Ygartue, K. Konjuh, Sh. Schumann, K.M. Williams, and D. Mordo, “Monitoring Optical Properties and Thickness of PECVD SiON Anti-Reflective Layer by Spectroscopic Ellipsometry”, SPIE Microlithography XI, 3050 (1997) 602–606.

[14] H.H. Tompkins, St. Smith, D. Convey, R,B. Gregory, M.L. Kottke, and D. Collins, “Determining the Amount of Si-Si Bonding in CVD Oxynitrides”, Surf. Interface Anal. 35 (2003) 136–140.

[15] P.H. Berning, “Theory and Calculations of Optical Thin Films”, Physics of Thin Films, vol.1, pp.69–121, Academic Press, (1963).

[16] O.S. Heavens, “Optical Properties of Thin Solid Films”, Butterworths, 1955.

[17] H.H. Hopkins, “On the Diffraction Theory of Optical Images”, Proc.Roy.Soc., A 217, 1953, p. 408.